11th Australasian Fluid Mechanics Conference
University of Tasmania, Hobart, Australia
14-18 December 1992

SEDIMENTATION VELOCITY OF SOME COMPLEX-SHAPED PARTICLES IN NEWTONIAN AND NON-NEWTONIAN LIQUIDS

V. ILIC, J.J. VINCENT, R. ZHANG and N. PHAN-THIEN

Department of Mechanical Engineering
University of Sydney, NSW 2006, AUSTRALIA

ABSTRACT

The overall objectives of the work reported here were to benchmark numerical predictions using the boundary element method against experimental data for complex shaped particles sedimenting in Newtonian and in non-Newtonian liquids (contained in square and circular tanks, respectively) as well as to ascertain the effect of a particle's shape on its settling velocity.

Using a dimethylpolysiloxane (silicone oil) and a 3% (w/w) aqueous solution of polyacrylamide, sedimentation tests were performed with a series of single particles having different shapes but the same volume and/or surface area.

The experimental and numerical results show good agreement for the Newtonian test liquid, but appreciable deviations were found for the non-Newtonian test liquid. In the Newtonian liquid, deviations in the sedimentation velocity due to particle shape were observed to be up to 15%.

INTRODUCTION

Understanding the settling of heavy particles of arbitrary shape in liquids is required for efficient process design and in the manufacture of new material composites, such as reinforced plastics, cermets, solid fuel propellants and explosives. Applications may also be found in mineral processing, handling of sewage, and silting of river estuaries.

The sedimentation in Newtonian liquids of spherical particles, either singly or in clusters, is well understood and has been modelled accurately with the boundary element method (BEM) (Ingber 1990), with the completed double layer boundary integral method (Phan-Thien et al. 1992) and with 'Stokesian Dynamics' (Brady and Bossis, 1988). However, there appears to be no similar information in the published literature on the sedimentation of particles having other shapes in either Newtonian or non-Newtonian liquids.

In general, the characteristic feature of the sedimentation process is a low Reynolds number flow, such that the Navier-Stokes equations reduce to the Stokes equations of motion,

$$-\nabla P + \mu\nabla^2\mathbf{u} = 0, \;\; \nabla\cdot\mathbf{u} = 0, \;\; \mathbf{x}\in\mathcal{D}, \qquad (1)$$

where $\mathbf{u}$ is the velocity field, P is the hydrostatic pressure, μ is the constant viscosity, and $\mathcal{D}$ is the domain of interest, ie., the fluid volume between the container and the particle surface.

In the case of non-Newtonian fluids, the equations of motion (which now contain a non-Newtonian term as a pseudo body force) are solved iteratively for the velocity field, also using the BEM formulation, following the assumption of a relevant constitutive equation.

The objectives of our work were to benchmark the numerical predictions using the boundary element method against experimental data for complex shaped particles sedimenting in Newtonian and non-Newtonian liquids (contained in square and circular tanks, respectively) and to ascertain the effect of a particle's shape on its settling velocity.

PREVIOUS WORK

Most of the reported work on sedimentation deals with spherical particles, well documented in Happel & Brennan (1986), reflecting the early theoretical approach of Stokes (1851) who formulated the classical expression for the settling velocity of a spherical particle in an infinite fluid.

However, in most practical applications, sedimentation takes place in a bounded fluid, such that the Stokes equations have to be 'corrected' to allow for the effect of the boundaries. In addition, particle shapes are usually non-spherical in practice and numerical methods must be used as there are no general analytical solutions available.

The application to geometrically complex-shaped multiple particles was made by Vincent et al. (1991), but without concomitant experimental verification. Some early systematic experimental data on the sedimentation of complex shapes was provided by Pettyjohn et al. (1948) and McNown & Malaika (1950). The particle size was varied in both studies.

In non-Newtonian fluids, the existence of three dimensional stress fields, time, rate and deformation effects necessitated formulation of numerous constitutive equations (Tanner, 1988). Using the BEM, numerical studies of a single sphere settling along the centreline of a cylinder were done by Zheng et al. (1990). A comparison of their results with experiments of Sigli and Coutanceau (1977) indicated the importance of mesh size and constitutive model chosen in their solution. As far as can be ascertained from the published literature, there does not appear to be any systematic study of the sedimentation of complex shapes in viscoelastic fluids.

METHOD

Experimental

Test shapes, conduits and liquid. The shapes used were spheres, cones, double cones, cylinders, long cylinders, tetrahedra, double tetrahedra, square pyramids, double square pyramids and cubes. All shapes had aspect ratios between 1:1 and 2:1 except the long cylinder which had an aspect ratio of 10:1. Their size was based on having either surface area or volume equal to that of a 20mm diameter sphere. All the particles were made from aluminium (specific gravity 2.8).

The experiments with the non-Newtonian liquid were conducted in a circular cylinder, while a square conduit was used for tests with a Newtonian test liquid. Both tanks had quiescent liquid in them and had their bottom end closed, while the upper surface of each cylinder was open to the atmosphere. The open end accommodated a removable lid containing the test particle releasing fixture ensuring precise axial drops.

The circular conduit (50.4 mm bore x 350 mm deep) was made from 4 mm thick glass and the large square conduit (200 x 200 x 900 mm) from 10 mm thick (fish tank) glass plates. Vertical alignment of the tanks was made with a spirit level and a plumb line. Two video cameras were used to record the start and finish of a settling particle traverse. Each camera was levelled with the timing mark in the centre of its field of view with the aid of an in-built spirit level.

The Newtonian test liquid was Gensil 150/12500 dimethylpolysiloxane (silicone oil) manufactured by the Bevaloid Australia Pty Ltd. The specific gravity of this liquid was 0.974 (measured with a 900/1000 S & B Hills Pty Ltd hydrometer) and the viscosity 14.5 Pa s (measured with a PSL 1619/8 BS/U size H capillary viscometer). Both measurements were made at 20.0°C.

The Newtonian nature of the fluid as well as the temperature dependence (in the range 10 − 30°C) of its viscosity were determined, up to shear rates of 34 s^{-1}, with an Instron 3250 rheometer and a water cooled Carri-Med controlled stress rotating cone rheometer, respectively. The obtained values for viscosity at 20.0°C agreed well with those obtained using a capillary viscometer.

The non-Newtonian test liquid used in the circular cylinder was a 3%(w/w) aqueous solution of polyacrylamide (Separan). The apparent viscosity of this liquid was measured with a Carri-Med controlled stress rotating cone rheometer at shear stresses up to 400 Pa and was verified with an Instron 3250 rheometer.

The liquid temperature was controlled by the environmentally controlled laboratory atmosphere to within ±1.0°C.

Apparatus, Data Collection and Processing. At the start of an experiment, the particle to be dropped was held by vacuum in the required position in the test conduit fixture lid and, prior to its release, was partially immersed in the tank liquid.

Two video cameras (Panasonic WV-BL200) with 420 horizontal line resolution at the centre, were each fitted with a Computar lens (f= 1:1.2, 12.5 - 75 mm zoom) and focused at timing markers on the outside of the top half of the conduit. The cameras were mutually orthogonal, and each conveyed a signal to a video splitter (American Dynamics 1470A). The video splitter was used to provide a simultaneous view of the two images on the monitor (National WV-5410E/A) screen whose resolution was more than 850 lines at the centre. The displayed combined image was recorded on a SVHS VCR (Panasonic NVFS 100A). Superimposed on the combined image was the test time (to one hundredths of a second) from the National time generator WJ-810.

Using the VCR single frame advance facility, the particle terminal velocity was then evaluated from the known distance between the two timing markers on the test cylinder and the time taken to traverse it.

It is estimated that the experimental error for the settling velocity is < 2% on the basis of the uncertainties in the measurements of time and distance.

Numerical

The boundary element method was used to model these sedimenting particles. This was implemented by Tullock (1992).

The boundary $\partial\mathcal{D}$ is divided into a series of M elements over which the geometry, velocity and traction are approximated by piecewise polynomials, such that the velocity and traction over an element can be expressed by

$$u_j = N^\alpha u_j^\alpha, t_j = N^\alpha t_j^\alpha \quad (2)$$

where $N^\alpha, \alpha = 1 \ldots n$, is the interpolation shape polynomial (shape function), u_j^α is the jth component of the velocity, $t_j^\alpha = n_i\sigma_{ij}$ is the jth component of the traction and n_i is the surface normal at node α. It can be shown that the boundary integral equation equivalent of the governing equations, becomes, in discretised form,

$$C_{ij}(\mathbf{x})u_j(\mathbf{x}) = \sum_{q=1}^{M}\left\{\left(\int_{S_q} u_{ij}^*(\mathbf{x},\mathbf{y})N^\alpha dS(\mathbf{y})\right)t_j^\alpha - \left(\int_{S_q} t_{ij}^*(\mathbf{x},\mathbf{y})N^\alpha dS(\mathbf{y})\right)u_j^\alpha\right\} \quad (3)$$

This equation, applied to a series of collocation points α (usually the nodes) over the boundary, leads to a set of linear algebraic equations.

The particle is given a unit velocity in the direction of and about each of the Cartesian axes individually. The corresponding nodal velocities are substituted into (3) which is then solved for the nodal tractions. These tractions are used to calculate the force and torque components on the particle. The resulting set of six equations are inverted to give an expression for the linear and angular velocity components in terms of the actual applied force and torque.

For the numerical simulation of the non-Newtonian sedimentation, an inelastic model with a Carreau viscosity function was used because the effective viscosity was expected to have the greatest effect on the sedimentation velocity (Bird 1977) and because the Carreau viscosity function fits the flow curve of the polyacrylamide solution (measured with a Carri-Med viscometer) very well.

Numerical calculations for flows with inertial and/or non-Newtonian effects are more complex mainly due to the non-linearity of the governing equations, and hence must usually be solved iteratively as a perturbation to a base Newtonian Stokes flow detailed above. The inertia term and/or the non-Newtonian stress components will give rise to a pseudo body force term. The development of an integral equation then follows the standard method described in elasticity or fluid mechanics (e.g. Brebbia 1980). However, a domain integral term will appear in the boundary integral formulations. The domain integral can be evaluated using numerical quadrature techniques (used here), or can be removed using some recently developed approaches (see for example, Zheng et al. 1991).

Another difficulty associated with the inertia and/or non-Newtonian flows arises from the formation of steep velocity and stress boundary layers near the particle surface as the Reynolds number and/or the Weissenberg number (in viscoelastic flow cases) increase. Therefore inadequate discretization may cause incorrect numerical results. In order to obtain reliable results economically, the finite element mesh used varied in density being fine near the particle surface and coarse elsewhere. A typical mesh for a falling spheroid is given in Fig. 1. Several meshes with varying degree of coarseness were used in the calculations to test convergence with mesh refinement. Despite the saving with this graded mesh, the limited computer capacity available required a smaller axisymmetric domain, so a cylindrical tank of 50.4mm bore was used.

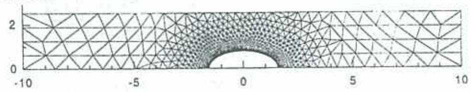

Fig. 1: A typical mesh used to evaluate the domain integral in non-Newtonian liquid.

RESULTS AND DISCUSSION

The results for Newtonian fluids are shown in Figs 2, 3 and 4. Figs 2 and 3 have both experimental and BEM results. The close agreement is immediately apparent with most differences being less than 2%.

Results for different shaped particles all with the same surface area are shown in Fig. 2. The terminal velocities are divided by that of a sphere with the same surface area. As expected the particles with the largest volumes (the sphere and the double cone) fall faster than those with the lowest volumes (the long cylinder), regardless of the particle shape. The broken line represents the calculated velocity of a sphere with the same surface area but a force applied to it corresponding to the volume of the different particles. A particle's deviation from this line therefore represents how its velocity is affected by its shape rather than by its weight.

The behaviour of the different shaped particles having the same volume and therefore the same applied force is shown in Fig. 3. The terminal velocities of the settling particles are divided by that of a sphere with the same volume. Again, the expected result is observed with the particles having the largest surface areas falling more slowly. The broken line represents the calculated velocity of a sphere with the same applied force and with a surface area equal to that of the different particles. A particle's deviation from this line again represents how its velocity is affected by its shape rather than by its surface area.

Experimental results for different shapes with different surface areas and volumes are shown in Fig. 4. The velocity per unit applied force has been normalised against a sphere with the same surface area and has been plotted against the normalised vertical projected area (projected onto a horizontal plane). The main observations to be made here are the three linear relationships, one for particles with a point at each end, another at a lower velocity for those with a point at one end, and a third at an even

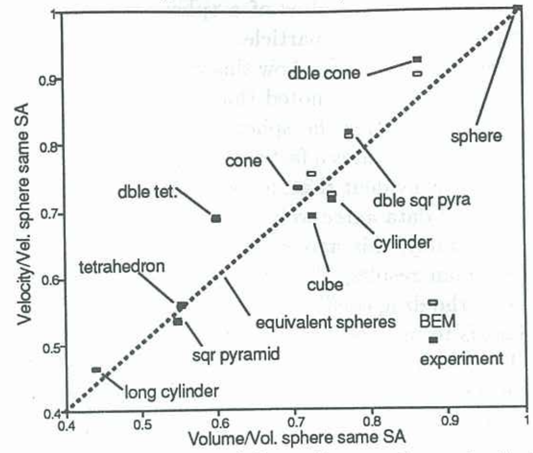

Fig. 2: The variation of the sedimentation velocity in a Newtonian liquid for shapes with the same surface area.

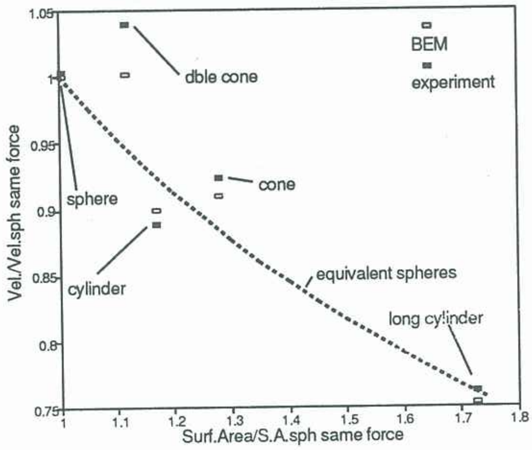

Fig. 3: The variation of the sedimentation velocity in a Newtonian liquid for shapes with the same volume.

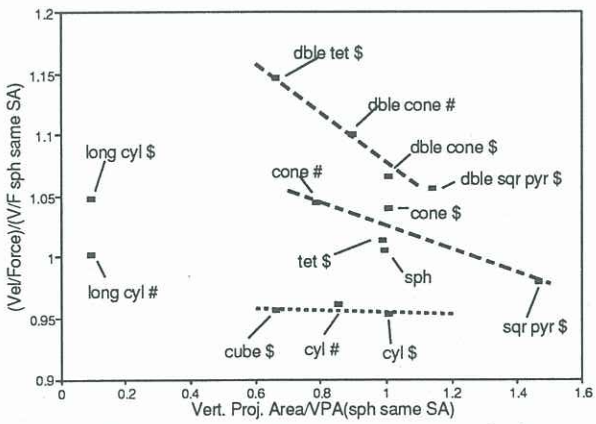

Fig. 4: The variation of the sedimentation velocity per unit force in a Newtonian liquid for shapes with either the same volume(#) or the same surface area($) as a 20mm diameter sphere.

lower velocity for those which are flat at both ends.

In the small circular tank required for the non-Newtonian tests, the wall effect was appreciable. Data for tests in Newtonian and non-Newtonian liquids using shapes of the same surface area are given in Table I. These are expressed in terms of a drag coefficient, $F/(6\pi\eta UR)$, where F denotes the drag force on the particle, η is the zero-shear-rate viscosity, U is the terminal velocity of the particle and R is the radius of a sphere which has the same surface area as the particle.

The Newtonian results show this wall effect for each of the shapes; it should be noted that, without wall effects the drag coefficient for the sphere would be 1. A small drag coefficient indicates a fast sedimentation velocity per unit force. It is evident that, as before, the experimental and numerical data agree well.

Unfortunately, this agreement does not apply to the non-Newtonian results. The numerical data indicate a decrease in the drag coefficient relative to the Newtonian case. This is to be expected from the effect of shear thinning. The Carreau model used in the calculations does not allow for elasticity, which may, in part, account for the discrepancy between these results and those obtained experimentally. Elasticity has the greatest effect with elongational flow, as found particularly around particles with flat ends: the cone and the long cylinder in this case.

Table I: Drag coefficients of particles of the same surface area sedimenting in a 50.4 mm bore cylinder.

shape	Newtonian		non-Newtonian	
	experimental	numerical	experimental	numerical
sphere	3.57	3.536	0.897	1.034
cone	3.21	3.167	1.24	0.9869
double cone	3.12	3.012	0.814	0.9186
spheroid	2.67	2.731	0.627	0.9116
long cylinder	2.12	2.153	1.010	0.6441

CONCLUSIONS

The settling velocity of a complex shaped particle sedimenting in a square tank (side length/sphere diameter ratio 10:1) containing a Newtonian liquid showed a deviation of up to 15% relative to an equivalent sphere. Irrespective of particle surface areas or volumes, there appeared to be a tendency for grouping related to particles' symmetry: shapes with pointed ends settled faster (per unit force) than those with flat end surfaces. The sphere and shapes with one flat and one pointed end had an intermediate settling velocity. Long cylinders settling endwise did not fall into any such group.

The non-Newtonian numerical data in a cylindrical tank (tank bore/sphere diameter ratio 2.5:1) showed only a qualitative agreement with experimental results owing to, in part, the combined effect of shear thinning, elasticity and wall effects. Fluid models allowing for elasticity as well as viscosity should be tried in future studies. The experimental data also indicate that, per unit force, flat ended particles sediment more slowly than those which are streamlined.

ACKNOWLEDGEMENTS

This work was supported in part by a Sydney University Special Projects Grant and the Australian Research Council Grant. The authors are also grateful to Alcan Australia Ltd, Bevaloid Australia Pty Ltd, BP Chemicals Ltd, Goodman Fielders Mills Ltd, Oral-B Laboratories Pty Ltd, RMAX, SKF Australia Pty Ltd, and Tioxide Australia Pty Ltd, for their support in kind.

REFERENCES

BIRD, R B, ARMSTRONG, R C and HASSAGER, O (1977) Dynamics of polymeric liquids, I. John Wiley & Sons.

BRADY, J F and BOSSIS, G (1988) Stokesian dynamics. Ann Rev Fluid Mech, 20, 111-157.

BREBBIA, C A (1980) The boundary element method for engineers. Pentech press, London.

HAPPEL, J and BRENNER, H (1986) Low Reynolds number hydrodynamics. Martinus Nijhoff Publishers, Boston.

INGBER, M S (1990) Dynamic simulation of the hydrodynamic interaction among immersed particles in Stokes flow. Int J Num Meth Fluids, 10, 791-809.

McNOWN, J S and MALAIKA, J (1950) Effects of particle shape on settling velocity at low Reynolds numbers. Trans American Geophysical Union, 31(1), 74-82.

PETTYJOHN, E S and CHRISTIANSEN, E B (1948) Effect of particle shape on free-settling rates of isometric particles. Chem Eng Prog 44(2), 157-172.

PHAN-THIEN, N, TULLOCK, D, ILIC, V and KIM, S (1992) Completed double layer boundary element method: a numerical implementation and some experimental results. (To be published in Computational Mechanics).

SIGLI, D and COUTANCEAU, J (1977) Effect of finite boundaries on the slow laminar isothermal flow of a viscoelastic fluid around a spherical obstacle. J Non-Newtonian F Mech 2, 1-21.

STOKES, G G (1851) On the effect of the internal friction of fluids on the motion of pendulums. Trans Cambridge Philos Soc, Pt. II, 9, 8-27.

TANNER, R I (1988) Engineering rheology. Oxford University Press.

TULLOCK, D (1992) PhD thesis (in progress), Department of Mechanical Engineering, The University of Sydney.

VINCENT, J, PHAN-THIEN, N and TRAN-CONG, T (1991) Sedimentation of multiple particles of arbitrary shape. J Rheol 35(1), 1-27.

ZHENG, R, PHAN-THIEN, N and COLEMAN, C J (1991) A boundary element approach for non-linear boundary value problems. Computational Mechanics, 8, 71-86.

ZHENG, R, PHAN-THIEN, N and TANNER, R I (1990) On the flow past a sphere in a cylindrical tube: limiting Weissenberg number. J Non-Newtonian F Mech, 36, 27-49.